

# Instantaneous Cycle-Slip Detection and Repair of GPS Data Based on Doppler Measurement

Zhoufeng Ren, Liyan Li, Jie Zhong, and Minjian Zhao

**Abstract**—In GPS receivers, carrier phase measurement can be used to improve the receiver’s position accuracy. In order to maintain the accuracy, cycle-slip must be detected and repaired instantaneously and accurately. This paper first analyzes the implementation cycle-slip detection and repair method of GPS data based on Doppler measurement. Then introduce a simplified oscillator model. Based on the oscillator model, a modified method is proposed, which avoids the influence of the local oscillator bias. Data tests show that the root mean square error of the time-difference measurement residual based on the proposed method is small enough for detecting and repairing the cycle-slip instantaneously.

**Index Terms**—Cycle-slip, Doppler measurement, GPS data, instantaneous.

## I. INTRODUCTION

GPS is rapidly replacing most of the traditional surveying techniques and is widely used in daily life. This is due to the great flexible conditions of using this system, like no time limitation, un-necessity of inter-visibility and un-limitation for the separation between surveyed points, free of charge etc. With the continuous progress of GPS Modernization, the economy, high precision and high reliability of the GPS receiver has become more and more popular. In order to obtain accurate positioning, carrier phase measurement is usually used in positioning. In addition to the initial integer ambiguity of the carrier phase measurement, cycle-slip is still a big challenge compared with the pseudo-range measurements. Cycle-slip is discontinuity of an integer number of cycles in the measured carrier phase resulting from a temporary loss-of-lock in the carrier tracking loop of a GPS receiver. The causes of the cycle-slip are listed as below [1]:

- 1) Cycle-slip is caused by obstructions of the satellite signal due to trees, buildings, bridges, mountains, etc.
- 2) Cycle-slip is a low signal-to-noise ratio (SNR) or alternatively carrier-to-noise-power-density ratio (C/N0) due to bad ionospheric conditions, multipath, high receiver dynamics, or low satellite elevation angle.
- 3) Cycle-slip is a failure in the receiver software which leads to incorrect signal processing.

The occurrence of cycle-slip affects not only the current measurement, but also the following epochs. It seriously degrades the positioning accuracy. In order to attain constant

high-precision positioning result, cycle-slip must be detected and repaired or handled with carrier phase measurements at the data processing stage.

Currently, many methods are used to detect and repair cycle-slip, such as polynomial fitting, high-order difference method, combination method of pseudo-range and carrier phase, ionosphere residual method and so on[2]. But these methods have their own disadvantages: Polynomial fitting can be used for single or dual frequency measurements in post-processing, but it can’t be used in real-time cycle slip detection. High-order difference method can’t detect small cycle-slip, which is fit for post-processing. The ionosphere residual method must be used in dual-frequency receivers and cannot indicate on which channel the cycle-slip takes place. The combination method of pseudorange and carrier phase depends on the precision of pseudorange completely which can’t identify small cycle-slip.

Doppler measurement is the instantaneous change rate of carrier phase. It is a very robust measurement. Therefore, Doppler measurement is an alternative way to detect and repair cycle-slip. However, in practice, the oscillator is a non-ideal clock source. The deviation in oscillator may result in Doppler measurement error. The instantaneous clock deviation estimation is not an easy work. The oscillator’s error of the receiver will be appeared in the Doppler-aided cycle-slip detection and repair method (DCDRM). Based on the relationship between Doppler measurements and carrier phase measurements, this paper proposes a new method called modified Doppler-aided cycle-slip detection and repair method (Modified DCDRM), which avoids using the corrected Doppler measurements and actual integration time to detect and repair the cycle-slip.

## II. INSTANTANEOUS CYCLE-SLIP DETECTION TECHNOLOGY

### A. Doppler-Aided Cycle-Slip Detection and Repair Method

The carrier phase measurement equation can be written as[3]:

$$\begin{aligned} \Phi &= \Phi_u - \Phi_s + N \\ &= \frac{(r - I + T)}{\lambda} + \frac{c}{\lambda}(\delta t_u - \delta t_s) + N + \varepsilon_\phi \end{aligned} \quad (1)$$

where

$\Phi$  is the measured carrier phase;

$\Phi_u$  is carrier phase generated by receiver;

$\Phi_s$  is carrier phase arriving from satellite;

$\lambda$  is the carrier wavelength;

$r$  is the geometry range from receiver to GPS satellite;

Manuscript received January 6, 2012; revised February 9, 2011. The paper is supported by the Fundamental Research Funds for the Central Universities.

Z. Ren, L. Li, J. Zhong and M. Zhao are with the Department of Information Science and Electronic Engineering of Zhejiang University, China(e-mail: longgo2006@gmail.com; zhongjie@zju.edu.cn; eriklee@zju.edu.cn, mjzhao@zju.edu.cn).

$I$  and  $T$  are the delay of L1 carrier phase due to ionosphere and troposphere respectively;  
 $c$  is the speed of light;  
 $\delta t_u$  is the bias in receiver clock;  
 $\delta t_s$  is bias of the GPS satellite clock;  
 $N$  is the initial integer ambiguity;  
 $\varepsilon_\phi$  is phase noise. Make difference between adjacent epochs.

The time-difference measurement of carrier phase is described as:

$$d\Phi = \frac{(dr - dI + dT)}{\lambda} + \frac{c \cdot (d\delta t_u - d\delta t_s)}{\lambda} + dN + d\varepsilon_\phi \quad (2)$$

where

$d\Phi$  is the time-difference measurement between adjacent epochs;

$dI$  and  $dT$  are the variation of ionosphere and troposphere delay respectively;

$d\delta t_u, d\delta t_s$  is the variation of local, satellite clock bias;

$dr$  is the variation of geometry range from receiver to GPS satellite;

$dN$  is the cycle-slip.

Doppler measurement is immune from cycle-slip. So  $dr$  can be derived from Doppler measurements at adjacent epoch.

$$dr = \lambda \hat{\Phi}_d(k) = -\lambda \int f_{d0} dt \approx -\frac{f_{d0}(k-1) + f_{d0}(k)}{2} \lambda T_{sa} \quad (3)$$

where

$\hat{\Phi}_d(k)$  is the variation of geometry range from receiver to GPS satellite in the form of phase;

$f_{d0}$  is the true Doppler frequency;

$T_{sa}$  is the true integration time in GPS time.

As revealed in (2), the  $dr$  should be removed to estimate the size of the cycle-slip. Using the (3), the time-difference measurement residual (TDMR)  $\delta\Phi$  can be represented as:

$$\delta\Phi = d\Phi - \hat{\Phi}_d = dN + \varepsilon'_\phi \quad (4)$$

$$\varepsilon'_\phi = \frac{dr}{\lambda} - \hat{\Phi}_d - \frac{(dI + dT)}{\lambda} + \frac{c}{\lambda} (d\delta t_u - d\delta t_s) + d\varepsilon_\phi \quad (5)$$

The variation of atmospheric delay, satellite orbit bias, multipath, and receiver system noise are to be more or less below a few centimeters as long as the observation sampling interval is relatively short, which is much less than one cycle-slip. Once the TDMR of current epoch is much smaller or larger than the average of TDMR, we can say that there is a cycle-slip at current epoch.

Consider the first two moments of TDMR in (4):

$$E(\delta\Phi_k) = dN_k + E(\varepsilon'_{\phi k}), \quad k = 1, 2 \quad (6)$$

$$\text{Cov}(\delta\Phi_k) = \text{Cov}(\varepsilon'_{\phi k}) \quad (7)$$

where  $E(\cdot)$  and  $\text{Cov}(\cdot)$  are mathematical expectation and variance-covariance operators, respectively. Since there is no redundancy to carry out statistical testing in real-time operation for (6) and (7). They have to be calculated through adaptive estimation. The mean value of TDMR  $\delta\Phi$  and its root mean square error (RMSE)  $\sigma_k$  is

$$\bar{\delta\Phi}_k = \bar{\delta\Phi}_{k-1} + \frac{1}{k} (\delta\Phi_k - \bar{\delta\Phi}_{k-1}) \quad (8)$$

$$\sigma_k^2 = \frac{k-2}{k-1} \sigma_{k-1}^2 + \frac{1}{k} (\delta\Phi_k - \bar{\delta\Phi}_{k-1})^2 \quad (9)$$

where

$\bar{\delta\Phi}_k$  is the mean value of  $\delta\Phi$  from epoch 1 to  $k$ ;

$\sigma_k$  is the covariance of TDMR at epoch  $k$ .

The detection of cycle-slip is based on (10)

$$|\delta\Phi_k - \bar{\delta\Phi}_k| \leq p \cdot \sigma_k \quad (10)$$

where  $p$  is a scale factor of the threshold value which can define the ability to detect the cycle-slip.

When cycle-slip is detected, the next step is to determine its size. Cycle-slip can be repaired by the simplest way when the sampling interval is short enough. That is

$$dN = \text{round}(\delta\Phi_k - \bar{\delta\Phi}_k) \quad (11)$$

where  $\text{round}(\cdot)$  is a mathematical function which gets the nearest integer of the variable.

### B. Oscillator Model

As the local clock source is non-ideal, it will introduce the oscillator error into TDMR, making it much tougher to detect and repair small cycle-slip. An oscillator model has to be introduced into the modified DCDRM to avoiding the oscillator error.

The performance of frequency source is described by its accuracy and stability. Ideal oscillator stays at its nominal frequency in the life cycle. In fact, due to resonator aging, environmental influences such as vibration, temperature, pressure and humidity, will bring systematic bias and random error to frequency source. It can modeled as [4]

$$f(t) = f_0 + \Delta f + (t - t_0) \dot{f} + \tilde{f}(t) \quad (12)$$

where

$f_0$  is the nominal frequency;

$\Delta f$  is the frequency bias;

$\dot{f}$  is a frequency drift;

$\tilde{f}$  is a random frequency.

Reference [5]-[7] point out that ordinary oscillator has good stability in a short time. And the main error of the source is frequency bias. The oscillator model can be simplified as

$$f_a = f_n + \Delta f = (1 + \beta)f_n \quad (13)$$

$f_n$  is the nominal frequency;

$f_a$  is the actual frequency;

$\beta$  is a scale factor of the frequency bias.

The relationship of sampling interval  $T_{sn}$  which is timing at the nominal frequency and the actual time  $T_{sa}$  is listed:

$$T_{sa} = T_{sn} / (1 + \beta) \quad (14)$$

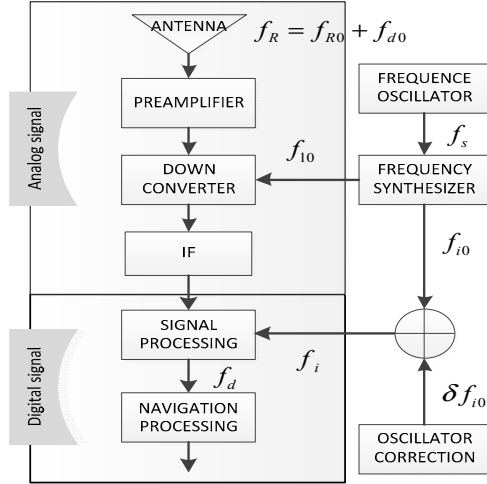


Fig. 1. Generic receiver functional block diagram.

### C. Modified DCDRM

System level functional block diagram of a generic receiver is shown in Fig.1. The generic receiver consists of the following 8 function blocks[8]: antenna, preamplifier, reference oscillator, frequency synthesizer, down-converter, an intermediate frequency (IF) section, signal processing and navigation processing. The radio frequency signal down-converts to intermediate frequency signal. And then in the digital signal part, the intermediate frequency converts to base band signal.

Consider an ideal oscillator model, which means  $f_s = f_n$ , then the oscillator correction will be zero. Then the Doppler measurement will be

$$f_d = f_R - f_{i0} - f_{i0} = f_R - f_{R0} = f_{d0} \quad (15)$$

where

$f_d$  is the Doppler measurement based on  $f_n$ ;

$f_R$  is the received satellite signal frequency, which contains the satellite sending frequency  $f_{R0}$  and the true Doppler frequency  $f_{d0}$ , and they satisfy  $f_R = f_{R0} + f_{d0}$

$f_{i0}$  and  $f_{i0}$  are the local oscillator frequency used to down-convert the satellite signal, the relationship is  $f_{i0} + f_{i0} = f_{R0}$ .

When the frequency source is not an ideal frequency source, according to (13), there will be a small deviation  $\Delta f$ , and  $f_s = (1 + \beta)f_n$ . All the frequency based on  $f_n$  will be biased. The relationship between the satellite signal and the local signal will be:

$$f_R = f_{R0} + f_{d0} = (1 + \beta)(f_{i0} + f_{i0} + \delta f_{i0} + f_d) \quad (16)$$

So the true Doppler frequency will be

$$f_{d0} = (1 + \beta)(f_{R0} + \delta f_{i0} + f_d) - f_{R0} \quad (17)$$

According to (1), TDMR can be expressed as

$$\begin{aligned} d\Phi(k) &= \Phi(k) - \Phi(k-1) \\ &= (\Phi_u(k) - \Phi_u(k-1)) - (\Phi_s(k) - \Phi_s(k-1)) \\ &= T_{sa}f_{R0} - (\Phi_s(k) - \Phi_s(k-1)) \end{aligned} \quad (18)$$

where

$\Phi_u(k)$ ,  $\Phi_s(k)$  are carrier phase generated in receiver and carrier phase arriving from satellite at epoch  $k$ ;

$T_{sa}$  is the actual sampling interval.

From (3) and (17),  $\hat{\Phi}_d(k)$  can be represented as

$$\begin{aligned} \hat{\Phi}_d(k) &= -\int f_{d0} dt \approx -\frac{f_{d0}(k-1) + f_{d0}(k)}{2} T_{sa} \\ &= -[(1 + \beta)(f_{R0} + \delta f_{i0} + \frac{1}{2}(f_d(k-1) + f_d(k))) - f_{R0}] \cdot T_{sa} \\ &= -(f_{R0} + \delta f_{i0} + \frac{1}{2}(f_d(k-1) + f_d(k))) T_{sn} + f_{R0} \cdot T_{sa} \end{aligned} \quad (19)$$

According to (18) and (19), we have

$$\begin{aligned} \delta\Phi &= d\Phi - \hat{\Phi}_d \\ &= (f_{R0} + \delta f_{i0} + \frac{1}{2}(f_d(k-1) + f_d(k))) T_{sn} - (\Phi_s(k) - \Phi_s(k-1)) \end{aligned} \quad (20)$$

From (20), we find that in the calculation of TDMR, it uses the raw data of carrier phase arriving from satellite, Doppler measurement based on  $f_n$  obtained from the signal processing block and the nominal sampling interval. It avoids correcting the local oscillator. And also it avoids introducing the oscillator error into the TDMR. It simplifies the computation and obtains a higher accuracy TDMR..

### III. DATA TEST

In order to illustrate the performance of our approach, we have tested it with data sets in static and kinematic modes. Static mode test is carried out in May 27, 2011 at Yuquan Campus of Zhejiang University, using a dual frequency receiver. Kinematic mode test is based on a signal simulator and the dual frequency receiver. Three dataset are collected in the test. The characteristic of the dataset is shown below:

- 1) Group one: It is a Static mode test. The receiver is fixed to place.
- 2) Group two: It is carried out in a uniform linear motion with a relative speed of -500 m/s.
- 3) Group three: It is carried out in a linear motion with a constant acceleration 2m/s<sup>2</sup>.

In static mode test, we chose PRN16 and PRN19 to analyze the performance of this approach. The SNR of PRN16 is about 40 dB-Hz, while the SNR of PRN19 is 49 dB-Hz. The mean value and the RMSE of TDMR are shown

in Table I.

In kinematic mode test, we chose PRN2 and PRN6 to analyze the performance. The SNR of this two satellite are both 42 dB-Hz. The mean value and the RMSE of TDMR are shown in Table II.

TABLE I: THE TDMR IN STATIC MODE TEST

Sampling interval (s)		0.1	0.5	1	2	10
PRN1 6	Mean (cycle)	0.0486	0.2455	0.4949	0.9858	5.2187
	RMSE (cycle)	0.025	0.0877	0.2066	0.5491	4.4399
PRN 19	Mean (cycle)	0.0466	0.2339	0.4751	0.9564	5.3310
	RMSE (cycle)	0.0140	0.060	0.1608	0.4726	4.116

TABLE II: THE TDMR OF THE GROUP TWO DATASET

Sampling interval (s)		0.1	0.5	1	2	10
PRN2	Mean (cycle)	0.0502	0.2494	0.5076	1.0239	5.008
	RMSE (cycle)	0.0261	0.1211	0.3238	0.9628	8.8139
PRN 6	Mean (cycle)	0.0498	0.2503	0.5077	1.0035	4.6852
	RMSE (cycle)	0.0256	0.1166	0.3226	0.9635	9.590

TABLE III: THE TDMR OF THE GROUP THREE DATASET

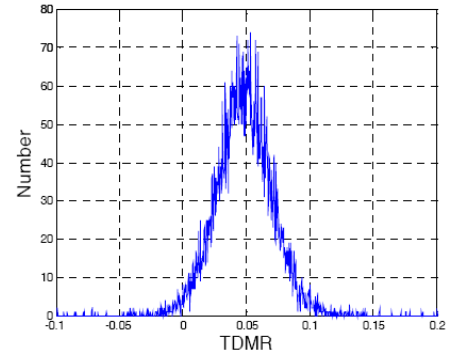
Sampling interval (s)		0.1	0.5	1	2	10
PRN2	Mean (cycle)	0.0307	0.1455	0.2879	0.5167	5.3695
	RMSE (cycle)	0.0299	0.1576	0.4670	1.1851	8.0266
PRN 6	Mean (cycle)	0.0584	0.2841	0.5659	1.0673	7.7096
	RMSE (cycle)	0.0300	0.1590	0.4684	1.1720	7.9484

Table I shows that the shorter the sampling interval is, the smaller the RMSE of the TDMR is. That is because time-difference measurement is not a linear function of Doppler frequency. It is an integration of the Doppler frequency. While in this method, an approximation is made by using the trapezoidal integration method, which makes the RMSE of TDMR increases larger as sampling interval increases. It's also shown that the RMSE of PRN19 is smaller than the RMSE of PRN16 at the same sampling interval, which is due to the larger SNR of PRN19.

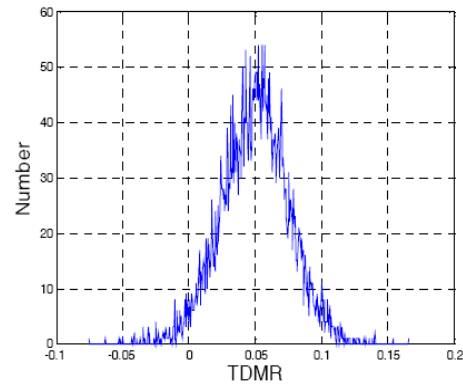
Compared with Table I, Table II and Table III show that the noise of TDMR in kinematic mode is significantly larger than in static mode at the same sampling interval. The same SNR of the different satellite almost have the same TDMR at the same sampling interval.

The distribution of TDMR without cycle-slip is shown in Fig.2, there are 5000 samples at 0.1s sampling interval in each graph. Fig.2 shows that the TDMR of the three tests satisfy none-zero means Gaussian distribution. Over 98.2%

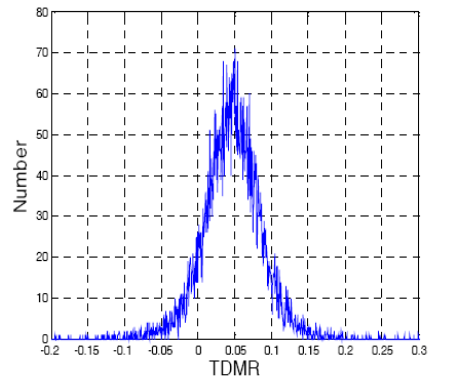
of the noise of TDMR is in 3 times  $\sigma_k$ . So we can set  $p$  to 3 in (10) to detect and repair the carrier phase cycle-slip. And then we found that the sampling interval must be smaller than 1 second to detect and repair one cycle-slip according to Table I Table II and Table III. And the small the sampling interval is the accuracy to detect and repair one cycle-slip is.



(a) The distribution of TDMR in group one.

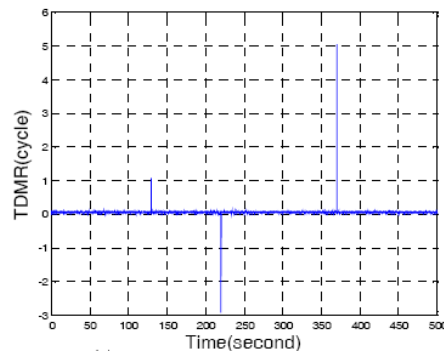


(b) The distribution of TDMR in group two.

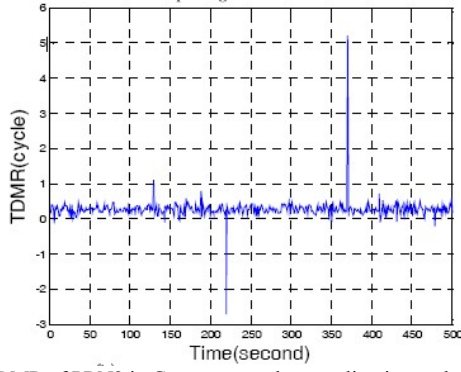


(c) The distribution of TDMR in group three.

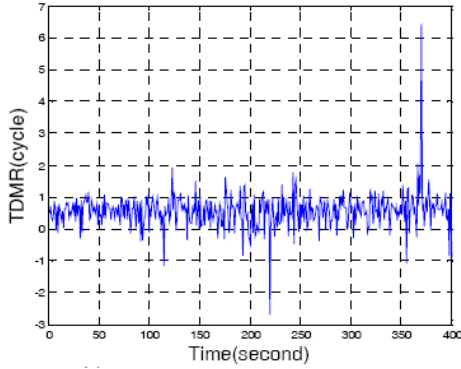
Fig. 2. The distribution of TDMR in static and kinematic mode.



(a) TDMR of PRN16 in Group one at the sampling interval of 0.1s.



(b) TDMR of PRN2 in Group two at the sampling interval of 0.5s.



(c) TDMR of PRN2 in Group three at the sampling interval of 1s.

Fig. 3. TDMR with cycle-slips at 130s 220s and 370s with different sampling interval.

To test this approach, we manually inserted 1, -3, 5 cycle-slips separately into the carrier phase measurements of PRN16 in Group one dataset at the sampling interval of 0.1 second, PRN2 in Group two dataset at the sampling interval of 0.5 second, and PRN6 in Group three dataset at the sampling interval of 1 second at the time of 130s, 220 second and 370 second. The TDMR of the satellites are shown in Fig.3.

Fig.3 shows that large cycle-slip are abrupt. We can detect them easily. The small cycle-slip may be buried in the noise at large sampling interval. As shown in Fig.3 (c), we can't identify the cycle-slip at the time 130 second. But we can find the cycle-slip in Fig.3 (a) due to the small sampling interval. When we detect the cycle-slip, we can use (11) to determine its size.

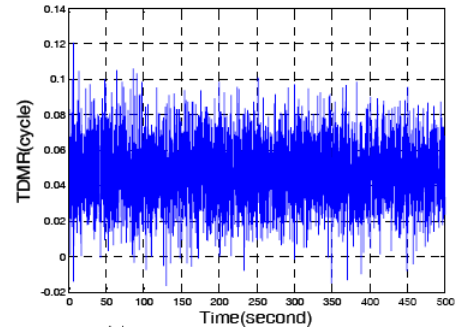
We use the proposed method to detect and repair the cycle-slip of the PRN16, PRN2 and PRN6. The results are listed in Table IV

Table IV shows that we detect and repair all the cycle-slips at the sampling interval of 0.1s and 0.5s. While at the sampling interval of 1s, we doesn't detect one cycle-slip at the epoch of 130s. It proves that if we want to detect small cycle-slip, the sampling interval must be smaller than 1 second. When the cycle-slips are repaired, the TDMR of the satellite are shown in Fig.4.

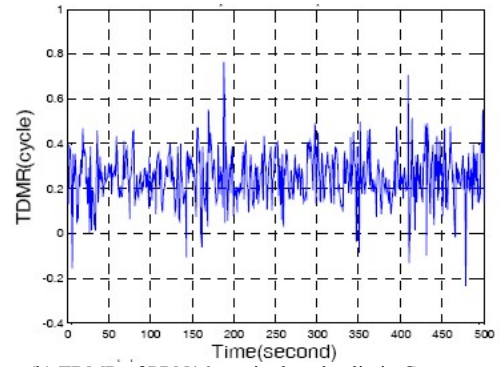
TABLE IV: RESULT OF THE APPROACH

PR N	EPOCH	TDMR	MEAN	RMSE	CYCLE-SLI
					P
16	130s	1.0773	0.0475	0.0187	1
	220s	-2.9239	0.0475	0.0184	-3
	370s	5.0307	0.0476	0.0179	5
2	130s	1.0935	0.2437	0.1008	1
	220s	-2.7314	0.2450	0.1171	-3

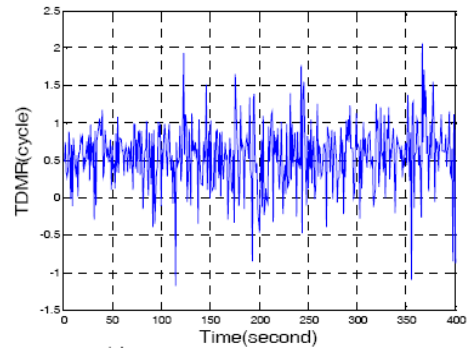
6	370s	5.1897	0.2511	0.1116	5
	130s	0.8954	0.5537	0.3893	0
	220s	-2.6840	0.5295	0.4285	-3
	370s	6.4331	0.5540	0.4452	5



(a) TDMR of PRN16 repaired cycle-slip in Group one.



(b) TDMR of PRN16 repaired cycle-slip in Group two.


 (c) TDMR of PRN16 repaired cycle-slip in Group two.  
 Fig. 4. TDMR of the satellite repaired cycle-slips.

#### IV. CONCLUSION

In this paper, we first analyze the implementation of DCDRM. Then a modified method is proposed based on a simplified oscillator model. In this method, the estimation of oscillator bias is removed. The test result shows that the mean value of TDMR is relatively robust, and its RMSE is rarely small at high sampling rate. The cycle-slip can be detected and repaired by rounding  $\delta\Phi_k - \overline{\delta\Phi}_k$  as long as sampling interval is short enough. Test result also shows that the RMSE of TDMR is larger in kinematic than in static mode. We can choose high sampling rate when the receiver is in kinematic mode.

ACKNOWLEDGMENT

The authors would like to acknowledge the excellent review of the entire manuscript by Zhaodi Liu.

REFERENCES

- [1] K. Donghyun and L.R. B, Instantaneous real-time cycle-slip correction for quality control of GPS carrier-phase measurements. Vol. 49. Manassas, VA, ETATS-UNIS: *Institute of Navigation*. 205-222. 2002.
- [2] L. Zhenkun, GPS dynamic cycle slip detection and correction with baseline constraint. *Journal of systems engineering and electronics*, 20(1): p. 5. 2009.
- [3] E. Kaplan, Understanding GPS: Principles and Applications, ed. S. Edition [M]. Boston: *Artech House Inc*. 2005.
- [4] P. Misra, Global Positioning System: Signals, Measurements, and Performance. Second Edition ed. 2006.
- [5] W. David Allan, N. A, and C. Clifford Hodge, *The Science of Timekeeping Application Note* 1289. 1997.
- [6] Y. Cao, Realization of GPS Satellite Time's Sampling and Verification of Local Time. *Electronic Technology*, 29(12): p. 3. 2002.

- [7] Y. Kou, a Method for Simulating the Crystal Oscillator Errors in GPS Receiver. *Journal of Electronics and Information Technology*, 26(8): p. 6. 2004.
- [8] W. Bradford Parkinson, J. J. S, *Global Positioning System: Theory and Applications*, Vol. I.



**Zhoufeng Ren** was born in Jingning, Zhejiang Province, China in 1984. He received his bachelor degree of Communication Engineering from Zhejiang University in 2007 China. After two year's work, he continues to study in college. He is currently a master student in Department of Information Science and Electronic Engineering of Zhejiang University, where he was doing research on GPS positioning and signal simulator.